PATTERNS OF ZONATION IN RARE-EARTH-BEARING MINERALS IN NEPHELINE SYENITES OF THE NORTH QÔROQ CENTER, SOUTH GREENLAND

IAN M. COULSON AND ANDREW D. CHAMBERS[1]

School of Earth Sciences, The University of Birmingham, Edgbaston, Birmingham B15 2TT, U.K.

ABSTRACT

The North Qôroq nepheline syenites form part of the rift-related Gardar Province of south Greenland. *In situ* fractionation of the syenitic magmas resulted in a peralkaline residual magma of lujavritic composition, with concentration of rare-earth elements (*REE*), Y, Zr and Nb. Such a residual magmatic liquid crystallized eudialyte, the major repository of these elements. Both syenites and country rocks were affected by metasomatism, associated with the intrusion and evolution of younger syenite units. From each new syenite, contrasting fluids evolved, commonly producing two compositionally distinct metasomatic events. Metasomatism associated with one of these fluids resulted in extensive redistribution of rare-earth and related elements, with apatite, titanite and fluorcarbonate minerals as the major repositories. These phases and the margins of primary eudialyte crystals show complex, cross-cutting patterns of zonation under back-scattered electron imagery and, in the case of apatite, cathodoluminescence. These patterns can be qualitatively related to successive pulses of metasomatic fluid containing variable concentrations of *REE*. In apatite, zoning involved the coupled exchange $Ca^{2+} + P^{5+} \rightleftharpoons REE^{3+} + Si^{4+}$, whereas in eudialyte and titanite, variation was less systematic, but involved Ca, Na, Si, *REE*, Y, Zr and Nb. The fluid responsible for the metasomatism must have been capable of transporting these elements and is considered to be rich in F^-, CO_3^{2-} and PO_4^{3-} and of probable carbonatitic affinities. It evolved from fractionating syenitic magmas at a late stage, probably as a result of liquid immiscibility.

Keywords: apatite, eudialyte, titanite, fluorcarbonate, metasomatism, rare-earth elements, North Qôroq, Igaliko, Gardar, Greenland.

SOMMAIRE

Les massifs de syénite néphélinique du centre igné de North Qôroq font partie de la province magmatique du Gardar, dans le sud du Groënland. Le fractionnement des magmas syénitiques *in situ* a donné un magma résiduel hyperalcalin de composition lujavritique, à forte concentration en terres rares (TR), Y, Zr et Nb. L'eudialyte a cristallisé à partir de ce magma évolué, et renferme la plus grande proportion de ces éléments. Une métasomatose, associée à la mise en place et à la cristallisation des venues tardives du magma syénitique, a affecté les venues précoces de syénite et les roches encaissantes. Des compositions distinctes de fluide se sont séparées de chacune des deux venues tardives. La métasomatose causée par une de ces vagues de fluide est responsable de la redistribution importante des terres rares et des éléments associés; l'apatite, la titanite et les fluorcarbonates en sont les minéraux hôtes importants. Ces cristaux tardifs et la bordure des cristaux primaires d'eudialyte témoignent d'une zonation complexe, avec zones non conformes, telles que révélées par la distribution d'électrons rétro-diffusés et, dans le cas de l'apatite, la cathodoluminescence. Ces zonations sont liées, de façon qualitative, à des infiltrations successives de fluide métasomatique contenant des concentrations variables de terres rares. Dans l'apatite, la zonation implique une réaction d'échange, $Ca^{2+} + P^{5+} \rightleftharpoons TR^{3+} + Si^{4+}$, tandis que dans l'eudialyte et la titanite, la variation est moins systématique, et semble avoir impliqué Ca, Na, Si, TR, Y, Zr et Nb. La phase fluide responsable de cette métasomatose doit avoir pu transporter ces éléments, aurait été enrichie en F^-, CO_3^{2-} et PO_4^{3-}, et serait probablement d'affinité carbonatitique. Cette phase fluide se serait séparée du magma syénitique par phénomène d'immiscibilité à un stade tardif de son évolution.

(Traduit par la Rédaction)

Mots-clés: apatite, eudialyte, titanite, fluorcarbonate, métasomatose, terres rares, North Qôroq, Igaliko, Gardar, Groënland.

---

[1] *E-mail address:* a.d.chambers@bham.ac.uk

INTRODUCTION

The North Qôroq center comprises a series of concentric nepheline syenite intrusions and forms part of the Igaliko Complex in the rift-related Gardar Province of South Greenland (Fig. 1). Recent reviews of this Proterozoic alkaline province by Upton & Emeleus (1987) and Macdonald & Upton (1993) contain descriptions of the regional characteristics, and field relationships and petrography of the North Qôroq syenites are given by Emeleus & Harry (1970).

In situ crystal fractionation has produced highly peralkaline (persodic), irregularly shaped bodies of lujavrite (a relatively fine-grained eudialyte-bearing syenite), similar to those described in the adjacent Motzfeldt center (Jones 1980, Jones & Larsen 1985). In such bodies, the primary magmatic processes have resulted in a concentration of rare-earth elements (*REE*) in the residual liquids. Later redistribution of the *REE* occurred through multiple metasomatic events (Rae *et al.* 1996). The minerals containing the bulk of the *REE* are eudialyte, apatite, titanite, rare-earth fluorcarbonates and, in smaller quantities, britholite-(Ce) and Ca–Na–*REE*–Ti–Zr–Nb silicates of the møsandrite, låvenite and wöhlerite series.

In this study, we examine four of these *REE*-bearing phases and relate the patterns of zonation and chemical variation to either primary crystallization or metasomatic activity.

GEOLOGY

Within the North Qôroq center are six major syenite units. These are designated SN1A to SN5 (Fig. 2) and are in a sequence with SN1A the first and SN5 the last to be intruded. All the syenite units of the center are considered to be broadly synchronous; the suite has been dated at approximately 1262 ± 55 Ma by the Rb–Sr method, with an initial ^{87}Sr/^{86}Sr ratio near 0.705 [Blaxland *et al.* (1978); recalculated with λ ^{87}Rb = 1.42 × 10^{-11} a^{-1}]. These rocks range in composition from marginally undersaturated augite syenite, through more highly evolved nepheline syenite to, locally, peralkaline lujavrite. The full range of this variation can be seen within individual units of the North Qôroq center and has been ascribed to *in situ* crystal fractionation (Chambers 1976). It is described more fully below.

Within the area, numerous examples can be found of syenite intruding syenite, and also of syenite intruding a range of country rocks. The latter include the gneissose granites and granodiorites of the Ketilidian Julianehåb Granite Complex, and a range of rift-related sedimentary and volcanic rocks, including quartzite and basaltic lavas. Both older syenite units of the North Qôroq center and a variety of country rocks occur as large raft-like xenoliths within younger syenites, and show the effects of widespread patchy metasomatic modification. Previous petrographic and geochemical studies of country rocks occurring at the margins of younger syenites have provided strong evidence of this infiltration of fluid and extensive alteration (Rae & Chambers 1988). Areas of metasomatized syenite are particularly associated with the intrusion of SN1B and SN5 and are indicated on Figure 2.

PETROGRAPHY, MINERAL ZONATION AND CHEMISTRY

We have examined in detail a number of *REE*-bearing mineral phases from the various units of the North Qôroq intrusive suite. These are apatite,
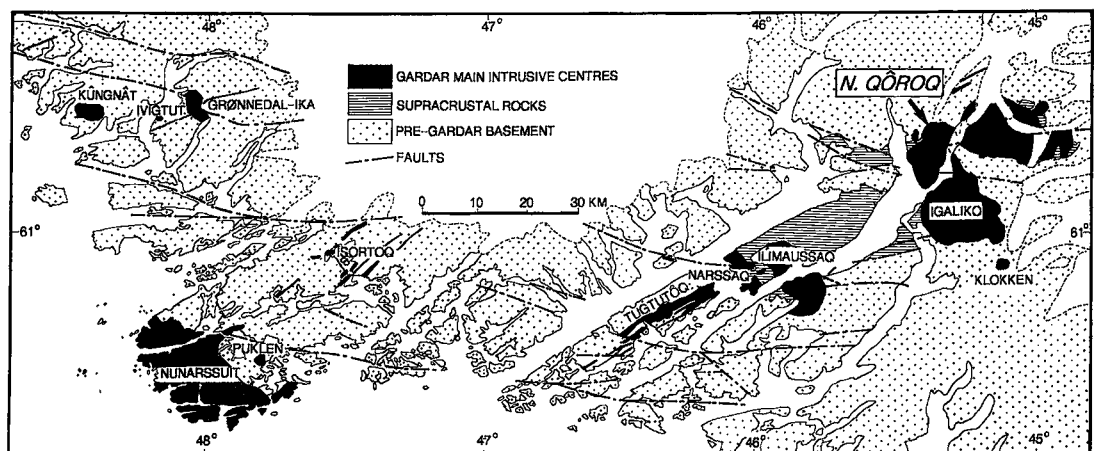
FIG. 1. Simplified map of the Mid-Proterozoic Gardar province, South Greenland, showing the major intrusive centers (after Emeleus & Harry 1970).
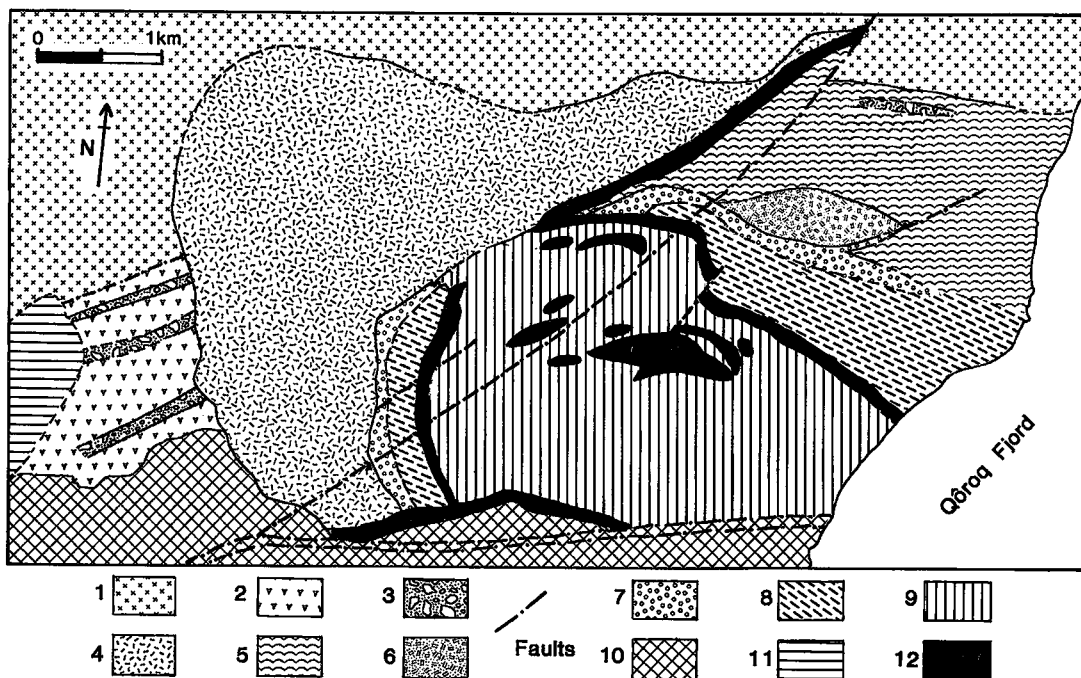
FIG. 2. Geological map of the North Qôroq center from the Igaliko Complex to the eastern margin of the Gardar province. Key: 1: Julianehåb Granite, 2 and 3: Supracrustal rocks, basaltic lavas and sediments, 4, 5, 6, 7, 8 and 9: Individual units constituting the center (SN1A, SN1B, SN2, SN4A, SN4B and SN5, respectively), 10: South Qôroq center, 11: Narsarsuaq nepheline syenite stock, 12: Principal areas of metasomatized syenites (modified after Rae & Chambers 1988).

eudialyte, titanite and rare-earth fluorcarbonate minerals; their petrography and mineral chemistry are described below.

Analytical methods

Cathodoluminescence images (CL) were obtained on polished thin sections, using a Technosyn cold-cathode luminescence instrument, model 8200 Mk II, attached to a Nikon Optiphot UFX–11 microscope and a Nikon FW–35WA camera at the University of Birmingham. The vacuum was provided by a Varian 5D–90 pump. An accelerating voltage of ~15 kV, current of 0.2 mA and a beam area of 1.5 mm^2 were used to study the sample.

Back-scattered electron images (BSEI) were obtained on an Oxford Instruments AN10/85S energy-dispersion spectrometer (EDS) system attached to a Cameca Camebax electron-probe microanalyzer instrument at the University of Edinburgh. Element X-ray maps were obtained from the same instrument using a beam current of 90 nA. The beam was scanned over an area of between 0.5 and 1.2 mm. The probe beam was moved over a 256 × 256 point grid with

counting intervals for X rays of 0.3 seconds over each spot. The brighter zones on the element maps correspond to higher count-rates.

The compositions of the minerals were determined using the same Cameca instrument in wavelength-dispersion mode. The operating conditions were: accelerating voltage 20 kV, beam current between 20 and 25 nA, a spot size in the region of 1 μm for titanite, and counting time of 30 seconds for each element (60–90 seconds for *REE* and fluorine). A rastered beam covering ~12 μm × 12.5 μm, within the bounds of spectrometer-focussing acceptability, was used for apatite, eudialyte and fluorcarbonate, which are susceptible to decay under the electron beam. Sodium was sought first, followed by other major elements to minimize artefacts due to decay.

Synthetic silicate glasses made at the University of Edinburgh were used as standards for the *REE*. These glasses are doped with between 15–20 wt.% of a single *REE* oxide, making them significantly richer in rare earths than the commonly used standards of Drake & Weill (1972). Lanthanum, Ce, Nd and Y were detected using *L*α lines, whereas for Pr and Sm, *L*β was used. Fluorine was detected using the second-order *K*α line

obtained with a PC2 synthetic multilayer crystal ($2d$ = 100 Å), so avoiding third-order $PK\alpha$ interference; higher-order interferences were removed using pulse-height discrimination. Data reduction was accomplished with full PAP correction procedures (Pouchou & Pichoir 1984). Samples exposed to an electron beam from cathodoluminescence studies were repolished before analysis (Stormer et al. 1993).

General petrography

Syenites from the North Qôroq center show extensive primary magmatic variation both within and between units. Within individual units, progressive and systematic petrographic changes can be seen across the outcrop. The least-fractionated areas of a syenite contain fayalitic olivine, ferro-augite, hastingsitic amphibole and Fe–Ti oxides, commonly occurring in mafic clusters and associated with apatite. Perthitic alkali feldspar, the dominant phase, shows exsolution on a fine scale, and feldspathoids are only present as interstitial grains (<5%). With progressive in situ fractionation (Chambers 1976), olivine disappears, the pyroxene become more sodic aegirine-augite, and the amphibole, Na-rich arfvedsonite. Feldspathoids are abundant, with nepheline, sodalite and cancrinite forming up to 40% of the rock. The most evolved areas of the syenite units are strongly peralkaline and include pegmatite and lujavritic rock-types. The lujavrites are relatively fine-grained, with pronounced feldspar lamination. Highly sodic pyroxene and amphibole dominate the mafic fraction, with eudialyte forming up to 20% of some rocks. In addition to feldspar, other felsic phases include nepheline, sodalite, cancrinite, analcite and natrolite.

Both within and around the North Qôroq center, changes in the petrographic character of both syenites and country rocks are indicative of metasomatic alteration (Rae & Chambers 1988). This alteration seems to be of two types, one resulting in alkali metasomatism, and the second characterized by the development of calcite and other Ca-rich phases including fluorite and apatite. Effects of both styles of metasomatism can be seen using conventional and cathodoluminescence petrography.

In metasomatized syenites, the first style of alteration results in mafic phases developing a strongly poikiloblastic rim, with aegirine-augite rimming ferro-augite and blue sodic amphibole rimming brown or green hastingsitic amphibole. Fe–Ti oxides are altered and rimmed by titanite or by aenigmatite, which can also occur as large poikiloblastic crystals. Feldspars are coarsely perthitic. Under CL investigation, those in unaltered rocks luminesce blue or purple, whereas metasomatism results in bright-red-luminescing albite (Rae & Chambers 1988). Sodalite occurs as a replacement mineral strongly embaying original euhedral nepheline. The second style of alteration is characterized by veins and patches rich in carbonate, fluorite and apatite, and by the poikiloblastic development of tiny (<20 μm) REE fluorcarbonate crystals.

The country-rock Julianehåb Granite is a two-feldspar gneissose granite where metasomatism has produced rocks that could be called fenite. The most obvious changes, as the contact with younger syenite is approached, is the grain-size reduction and eventual disappearance of quartz and the patchy growth of albite, alkali amphibole, alkali pyroxene and biotite. At the immediate contact, extensive metasomatism produced a rock with up to 90% modal albite. Cross-cutting this zone are later veins and patches containing calcite, fluorite, epidote and hydrogrossular-andradite garnet. Primary apatite occurs within the granite (<1%) but is more prominent in the calcite–fluorite veins and patches (3–4%).

Quartzitic sediments, originally almost pure quartz but now extensively altered, occur both as country rocks adjacent to the North Qôroq syenites and as xenolith rafts within the syenites. The first, more pervasive, alkali-rich style of metasomatism resulted in the development of extensive, interstitial, red-luminescing albite and in the patchy growth of alkali amphibole and pyroxene. A striking feature of the metasediments, attributed to the second style of alteration, is the development of mafic areas rich in more calcic pyroxene and amphibole, calcite, fluorite and large quantities (~20%) of apatite. Locally, a rim of apatite separates these mafic concentrations from areas of quartz and albite (Rae et al. 1996).

Where the altered country-rocks are basaltic, the alkali metasomatism resulted in extensive biotitization. Here also, a second metasomatic event produced veins and patches of calcite, fluorite, apatite, epidote and garnet surrounded by a diffuse zone containing diopsidic pyroxene and calcic amphibole.

The conclusion from the petrography is that metasomatic alteration generally involved an earlier, pervasive, alkali- and chloride-rich hydrous event, followed by more localized veins and patches due to the action of a Ca-, CO_3^{2-}-rich fluid with significant quantities of F^-, PO_4^{3-} and REE.

Apatite

Apatite occurs as both a primary (magmatic) phase and as a secondary (metasomatic) phase in the North Qôroq center. Primary apatite is most abundant in the least fractionated variant, augite syenite, where large crystals (up to 0.8 mm) occur as a major component (10 modal %) in mafic clusters associated with olivine, ferro-augite, hastingsitic amphibole and Fe–Ti oxides. It is also present in more fractionated batches of syenite, but in minor amounts (<1 modal %). These syenites show no petrographic evidence of meta-somatic alteration. In the Julianehåb Granite, apatite is

a minor primary phase (<1 modal %), but is more prominent in the cross-cutting calcite–fluorite veins and patches (3–4 modal %). In the quartzites, large quantities of apatite occur (up to 20 modal %) within the mafic areas, as small equant grains (<50 μm) within pyroxene, amphibole, calcite and fluorite; it is particularly concentrated in a rim (0.2 mm thick) that separates the mafic concentrations from mafic-mineral-poor areas.

Although no zonation is seen in apatite using conventional optical microscopy, examination by CL and BSEI records complex and striking patterns of zonation (Rae *et al.* 1996). In the North Qôroq syenites, primary apatite from rocks apparently unaffected by metasomatism commonly displays either yellow or buff-brown luminescence. The only zonation shown in apatite from this area is simple and concentric, consistent with crystallization and growth from an evolving magma.

Apatite from the fenitized and metasomatized rocks shows a greater complexity of zonation, with a number of irregular zones luminescing in shades of blue and purple. In some crystals, up to five distinct zones have been identified, with the outer zones commonly truncating and embaying earlier ones. Such patterns of multiple zonation are consistent with a series of metasomatic episodes affecting the apatite, each one probably associated with intrusion of a nearby syenite, from which a metasomatic fluid evolved.

BSEI results mirror the pattern seen in CL, and electron-probe analyses confirm that this zonation reflects variation in total *REE* content, with brighter zones (Fig. 3) having higher contents of *REE* and Si. Figure 3 shows X-ray maps of the same apatite crystal for Ce (*REE*), Si and Sr. These X-ray maps, together with results of electron-microprobe analyses, reveal that each zone is internally homogeneous, with consistent chemistry and without variation in *REE*
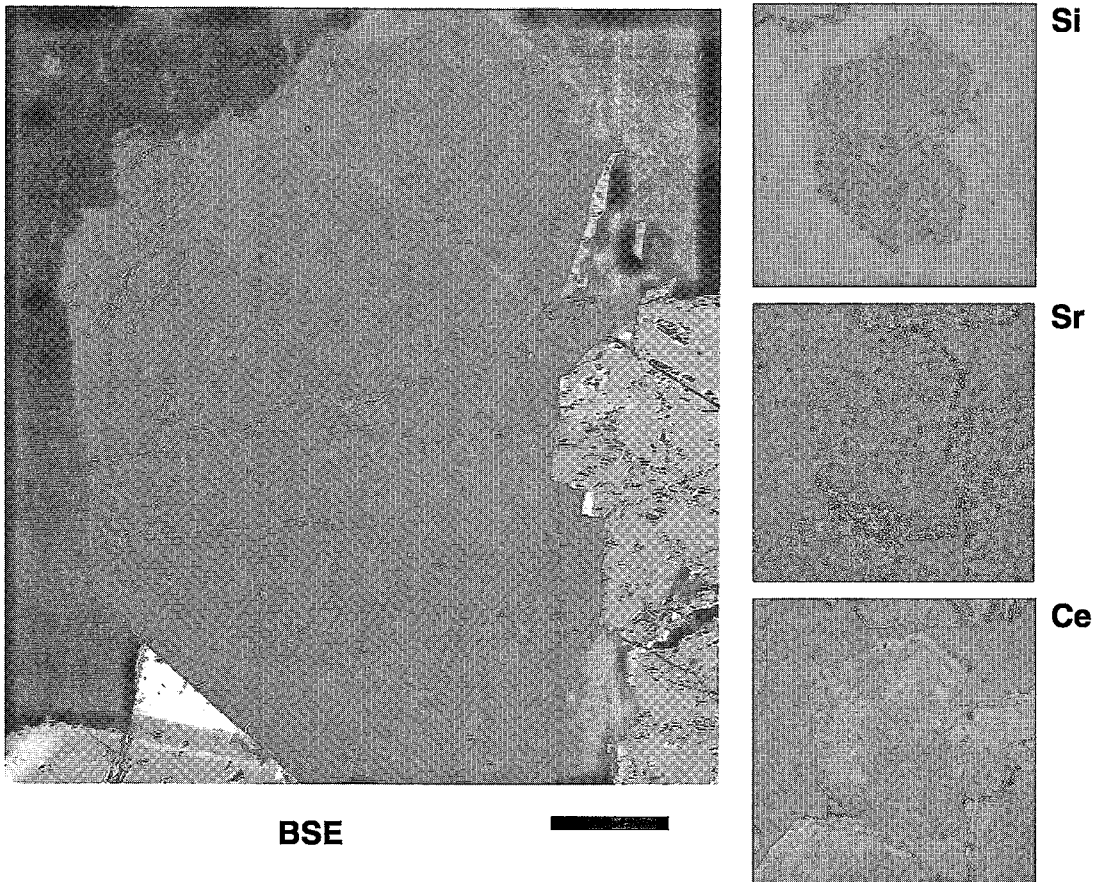
FIG. 3. Back-scattered electron image (BSEI) and corresponding X-ray maps for Si, Sr and Ce, illustrating the subtle but complex zonation in apatite from an evolved metasomatized North Qôroq syenite. Associated minerals in the BSEI are alkali feldspar (dark) and eudialyte showing zonation (light). Scale bar represents 100 μm.

TABLE 1. REPRESENTATIVE RESULTS OF ELECTRON-MICROPROBE ANALYSES OF APATITE FROM NORTH QÔROQ

Sample	DAR65 core	DAR65 rim	DAR67 rim	DAR67 rim	DAR163 core	DAR164 core	DAR167 core	DAR278 core	DAR278 rim	DAR301 core
Oxide wt.%	1	2	3	4	5	6	7	8	9	10
CaO	50.70	50.15	47.98	51.20	53.14	55.14	54.30	52.58	51.28	53.90
P_2O_5	39.75	39.08	36.30	39.78	40.32	42.17	41.44	41.93	39.98	41.87
SiO_2	1.37	1.59	3.21	1.25	1.36	0.36	0.75	0.60	1.43	0.39
FeO_{total}	0.19	0.12	0.41	0.11	<	<	<	0.14	<	0.24
MnO	n.d.	n.d.	<	n.d.	<	<	<	n.d.	n.d.	n.d.
SrO	1.53	1.62	1.04	2.03	<	<	<	<	<	1.00
Na_2O	0.34	0.22	n.d.	<	n.d.	n.d.	n.d.	0.17	0.18	0.12
La_2O_3	1.14	1.42	2.80	1.29	0.79	<	0.24	0.44	0.86	0.30
Ce_2O_3	1.78	2.27	4.22	1.60	1.68	0.23	0.73	1.03	2.10	0.43
Pr_2O_3	0.29	0.12	0.27	0.20	0.15	<	0.17	0.14	0.30	<
Nd_2O_3	0.70	0.82	1.43	0.48	0.65	0.12	0.39	0.54	1.06	0.15
Sm_2O_3	0.17	0.10	0.25	<	0.16	<	0.12	0.13	0.16	<
Y_2O_3	<	0.10	n.d.	<	n.d.	n.d.	n.d.	0.14	0.30	0.12
Cl	<	<	<	<	<	0.25	<	<	<	<
F	3.70	3.87	3.98	3.35	3.90	3.06	3.61	3.74	3.75	3.85
- O ≡ F, Cl	1.56	1.63	1.68	1.41	1.64	1.34	1.52	1.57	1.58	1.62
Total	100.09	99.86	100.23	99.87	100.51	99.97	100.23	100.01	99.90	100.81

Atomic proportions on the basis of 25 atoms of oxygen

P	5.81	5.76	5.47	5.81	5.81	5.97	5.91	6.00	5.83	5.97
Si	0.24	0.28	0.57	0.22	0.23	0.06	0.13	0.10	0.25	0.07
Ca	9.38	9.36	9.15	9.47	9.68	9.88	9.80	9.53	9.47	9.72
Fe	0.03	0.02	0.06	0.02	0.00	0.00	0.00	0.02	0.00	0.03
Mn	-	-	-	-	0.00	0.00	0.00	-	-	-
Na	0.06	0.04	-	0.00	-	-	-	0.03	0.03	0.02
Sr	0.15	0.16	0.11	0.20	0.01	0.01	0.00	-	0.00	0.10
La	0.07	0.09	0.18	0.08	0.05	0.00	0.01	0.03	0.05	0.02
Ce	0.11	0.15	0.27	0.10	0.10	0.01	0.04	0.06	0.13	0.03
Pr	0.02	0.01	0.02	0.01	0.01	0.00	0.01	0.01	0.02	0.00
Nd	0.04	0.05	0.09	0.03	0.04	0.01	0.02	0.03	0.07	0.01
Sm	0.01	0.01	0.02	-	0.01	0.00	0.00	0.00	0.00	0.00
Y	0.01	0.01	-	0.00	-	-	-	0.01	0.03	0.01

Sample numbers DAR65, DAR67 - apatite in quartzite; DAR163, DAR164, DAR167 apatite in granite-gneiss; DAR278 - apatite in syenite; DAR301 - apatite in basalt
n.d. = not determined; < below detection limit.

abundance.

Typical compositions of apatite, calculated on the basis of 25 atoms of oxygen, are given in Table 1 for a range of metasomatized rocks. Protoliths containing metasomatic apatite include gneissose granite, quartzite, basalt and syenite, although in the latter case, some compositions may pertain to magmatic compositions or contain an original magmatic component. A total of 150 analyses were made on 49 grains from 15 rock samples; a detailed study of the variation in cation and anion contents is presented elsewhere (Rae *et al.* 1996).

Apatite from the fenitized quartzite (*e.g.*, analyses 1–4) shows a significant departure from the formula $Ca_5(PO_4)_3(F,OH,Cl)$. In particular, concentrations of the *REE* can reach values up to 10.4 wt.% of the oxides, with a complementary increase in SiO_2. Strontium is also seen to substitute for Ca in the apatite structure. Figure 4 presents the compositional features of apatite in terms of the major cation components. The most significant substitution is a coupled one in which charge balance is maintained by Si^{4+} substituting for P^{5+} as REE^{3+} substitutes for Ca^{2+} (Sr^{2+}). Figure 4 shows that much of the variation in composition can be explained by this substitution, as all compositions (magmatic and metasomatic), no matter what the protolith, lie close to the theoretical line defining the substitution. In contrast, data points representing magmatic apatite from the nearby Ilímaussaq intrusion (Rønsbo 1989) fall well below this line owing to the importance of the exchange $2Ca^{2+} \rightleftharpoons Na^+ + REE^{3+}$. Sodium is absent or present at very low levels (<0.5 wt.% Na_2O) in apatite from the North Qôroq rocks, but it may be significant that the compositions departing most markedly from the line on Figure 4 pertain to apatite in syenitic host-rocks. This may indicate the presence of a primary magmatic component in the apatite from these rocks, involving a scheme of coupled substitution similar to that at Ilímaussaq.
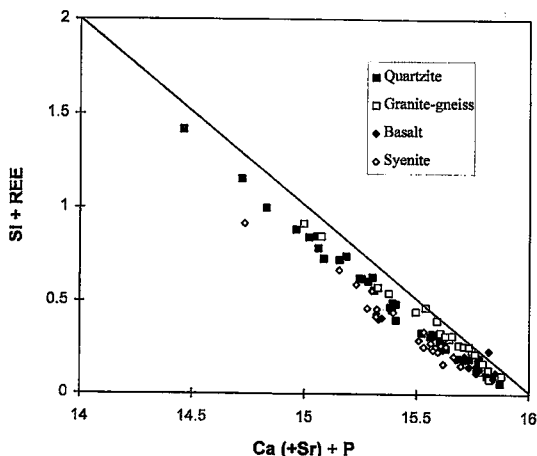
FIG. 4. Element variation shown by apatite from North Qôroq. Axes are plotted in cations per formula unit.

Eudialyte

Eudialyte reaches modal abundances of up to 20% in the most fractionated variety of syenite (the lujavrite) and late pegmatites, and occurs as idiomorphic (up to 1 mm) crystals commonly displaying alteration. Within these rocks, the eudialyte shows clear evidence of oscillatory zonation using conventional optical microscopy (Fig. 5a). From the same sample, small crystals of eudialyte and the margin of larger grains show more irregular patterns of zonation. In rocks showing clear evidence of alkali metasomatism, eudialyte occurs as large (>2 mm) grains in close association with sodalite, poikiloblastic sodic pyroxene, sodic amphibole and aenigmatite, all enclosing extensively albitized feldspar (Rae & Chambers 1988).

Figure 5a shows a single grain of eudialyte in cross-polarized light, and Figure 5b, the corresponding X-ray map for Ce. Identical patterns of zonation are present, indicating that the oscillatory zonation seen using conventional optical microscopy is mirrored by variation in REE abundance. The margins of eudialyte crystals are commonly resorbed, and the apparent linear pattern of oscillatory zonation is overprinted with irregular patches and embayments. This is clearly seen in Figure 5c, in which a BSEI of eudialyte shows a complex pattern of intracrystalline variation. The irregularity suggests that the oscillatory zonation, presumably a result of primary magmatic crystallization, is overprinted by metasomatic activity.

Representative compositions of eudialyte are given in Table 2; sixty-five analyses were made on 32 grains from six samples. Eudialyte is a problematical mineral

to analyze as it decays, if a spot beam is used, with loss of Na and increase in other elements. The analytical conditions outlined above minimized decay problems, and we believe that the compositions given in Table 2 are of good quality. Low totals, a common feature of eudialyte compositions, mainly reflects the presence of H_2O in the structure (up to 3 wt.%).

Recalculation of the analytical results presents another problem, as there is uncertainty as to the ideal formula (Giuseppetti et al. 1971, Harris & Rickard 1987). Probable partial site-occupancies, excess ions and water in spaces in the open framework, and extensive ionic substitutions, all render calculation of a structural formula problematical. In this study, $Na_3(Ca,REE)_2(Fe,Mn)Zr(Si_3O_9)_2(OH,Cl,F)$ has been used as the ideal formula of eudialyte. In view of the extensive substitution among cations, an anion base has been used, assuming 18.5 atoms of oxygen (equivalent to 19 O,OH,Cl,F).

Small degrees of variation occur in a number of elements, with systematic changes in levels of Na, Ca, Si and REE. Such changes are responsible for the oscillatory zonation seen in the crystals. Figure 6 shows these changes on an ionic basis. The level of Si is negatively correlated with Ca and positively correlated with Na. These trends are not artefacts of analytical decay-induced problems, as the decay process would produce correlations of Na and Ca with Si opposite to those observed. The levels of REE show a negative correlation with Si. For all the eudialyte samples analyzed, excluding the outermost rims, ZrO_2 seems consistent at between 11 and 12 wt.%, and Y_2O_3 is ~0.3 wt.%. Potassium, Al and Hf occurs in trace amounts, whereas other elements sought in the analyses (Ti, Ba, Sr, Cr and Mg) are below detection limits.

Superimposed on the chemical variation associated with oscillatory zonation are very weakly defined trends from core to rim. There is a general, slight increase in the level of Ca and REE, and a decrease in the level of Na and Si toward the rim. In addition, the proportion of Fe typically decreases, and that of Mn increases, toward the rim.

At the outermost rim of some crystals, more extensive variation is seen, particularly involving Nb and Zr. Niobium can reach values of nearly 6 wt.% Nb_2O_5, and Zr values can be much lower than the uniformly high values of the crystal interiors (see anal. 10 and 11, Table 3). This erratic variation, characteristic of crystal rims, is probably the result of metasomatic reactions at the grain margin, and implies that the fluid was capable of mobilizing Nb and Zr.

Titanite

Titanite is absent from the majority of North Qôroq syenite units, as Ti is preferentially incorporated into Fe–Ti oxides or aenigmatite and occurs as a minor
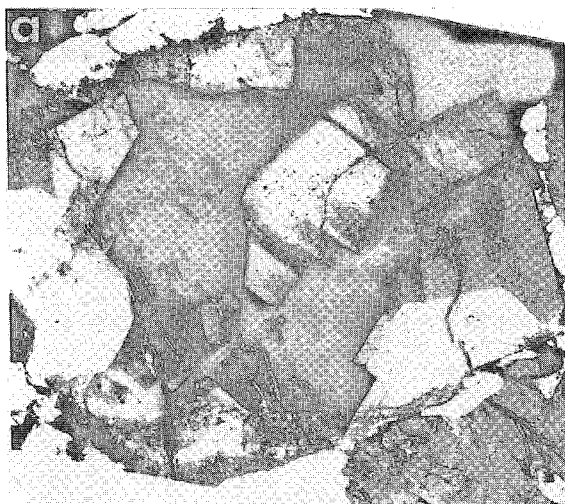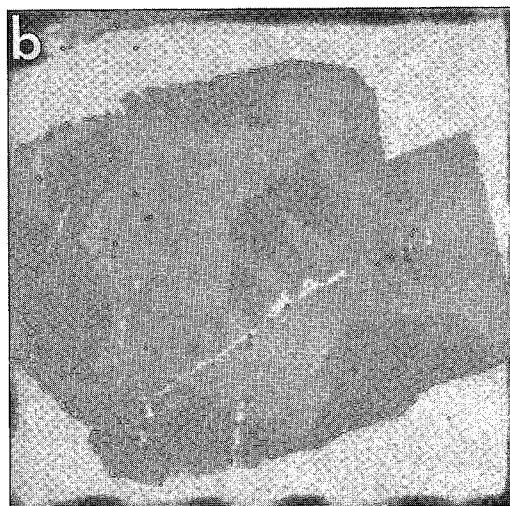
XPL   Ce X-ray map
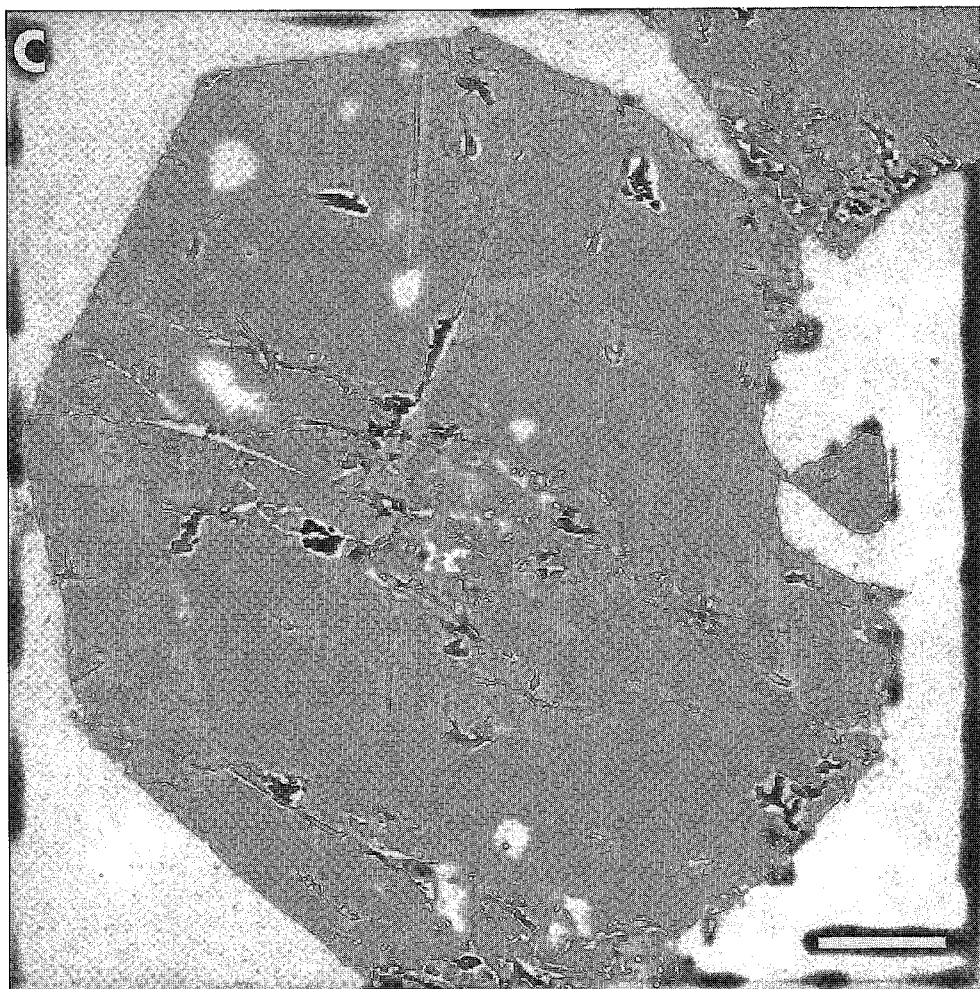
FIG. 5. Eudialyte from samples GGU59661 (pegmatite) (c) and DAR24 (lujavrite) (a and b): (a) complex patterns of zonation seen under crossed polars using conventional optical microscopy; (b) An X-ray map for Ce taken of the identical crystal. Scale bar for both represents 100 μm; (c) BSEI of eudialyte showing embayment of crystal margins and complex patterns of zonation along the margin. In each case, the eudialyte grains are surrounded by alkali feldspar, nepheline and cancrinite. Scale bar represents 50 μm.

←

component in pyroxene and amphibole. Titanite is present only in samples that show evidence of metasomatic alteration, commonly rimming Fe–Ti oxides. In the metasomatized country-rocks, titanite is more abundant (up to 15 modal %) and forms large clusters of idioblastic crystals, with individual grains attaining 1 mm in length and commonly associated with zircon.

BSEI of titanite show significant zonation (Fig. 7). Simple patterns of zonation in the center of grains are overprinted by more chaotic and irregular ones, particularly at the margins of crystals and along fractures. If the titanite is all of metasomatic origin, then this suggests that later metasomatic events have caused localized dissolution and changed the composition of the titanite.

Representative compositions of titanite from a variety of rock types from the North Qôroq area are reported in Table 3 (32 analyses were made on 20 grains from five samples). Structural formulae have been normalized on the basis of five atoms of oxygen using the method described in Deer *et al.* (1992), with ions allocated to octahedral, tetrahedral and seven-fold

TABLE 2. REPRESENTATIVE RESULTS OF ELECTRON-MICROPROBE ANALYSES OF EUDIALYTE FROM NORTH QÔROQ

Sample	DAR24 core	DAR24 core	DAR24 middle	DAR26 rim	59661[#] core	59661[#] middle	59661[#] rim	59663[#] rim	59663[#] core	DAR26 rim	59663[#] rim
Oxide wt.%	1	2	3	4	5	6	7	8	9	10[+]	11[+]
SiO_2	48.83	48.29	48.32	48.04	47.59	46.67	46.58	46.36	45.71	49.22	47.04
ZrO_2	11.92	11.79	11.77	11.61	11.63	11.44	11.00	11.69	11.38	11.56	6.94
HfO_2	n.d.	n.d.	n.d.	0.30	n.d.	n.d.	n.d.	0.23	0.18	0.26	0.12
Nb_2O_5	0.92	1.16	0.64	1.62	1.94	2.30	2.26	2.48	2.99	5.97	1.48
Al_2O_3	n.d.	n.d.	n.d.	0.23	n.d.	n.d.	n.d.	0.13	0.16	0.19	0.14
Y_2O_3	0.35	0.44	0.38	0.35	0.28	0.32	0.31	0.31	0.38	0.20	0.30
La_2O_3	0.42	0.51	0.42	0.57	0.35	0.55	0.60	0.62	0.80	0.47	0.56
Ce_2O_3	0.66	1.06	0.82	0.95	0.85	0.97	1.25	1.20	1.39	1.09	1.08
Pr_2O_3	0.12	0.10	<	0.10	0.12	0.09	<	0.31	0.13	<	0.13
Nd_2O_3	0.32	0.39	0.35	0.30	0.27	0.34	0.38	0.38	0.46	0.37	0.38
FeO_{total}	6.02	6.36	6.25	6.33	6.53	6.56	6.34	6.10	6.09	3.20	6.29
MnO	1.12	1.23	1.19	1.61	1.49	1.59	1.69	2.17	2.47	0.66	2.13
CaO	10.37	10.62	10.24	10.94	11.39	11.82	11.91	11.66	11.52	6.10	11.76
Na_2O	11.96	11.61	12.99	11.49	12.12	11.23	11.33	11.33	11.07	11.91	11.63
K_2O	0.20	0.19	0.18	0.19	0.15	0.28	0.29	0.23	0.25	0.39	0.24
F	n.d.	n.d.	n.d.	n.d.	n.d.	n.d.	<	n.d.	n.d.	n.d.	n.d.
Cl	1.46	1.40	0.95	1.38	1.23	1.29	1.29	1.34	1.24	0.88	1.12
-O ≡ F, Cl	0.33	0.32	0.22	0.31	0.28	0.29	0.29	0.30	0.28	0.31	0.25
Total	94.32	94.82	94.27	95.69	95.66	95.15	94.94	96.23	95.95	91.73	90.83

Atomic proportions on the basis of 18.5 atoms of oxygen

Si	6.44	6.38	6.39	6.34	6.26	6.21	6.22	6.17	6.12	6.54	6.45
Zr + Hf	0.77	0.76	0.76	0.76	0.75	0.74	0.72	0.78	0.75	0.76	0.48
Nb	0.05	0.07	0.04	0.10	0.12	0.14	0.14	0.15	0.18	0.36	0.09
Fe	0.66	0.70	0.69	0.70	0.72	0.73	0.71	0.68	0.68	0.36	0.72
Mn	0.13	0.14	0.13	0.18	0.17	0.18	0.19	0.24	0.28	0.07	0.24
Na	3.06	2.97	3.33	2.94	3.09	2.90	2.93	2.92	2.87	3.07	3.09
Y	0.02	0.03	0.03	0.02	0.02	0.02	0.02	0.03	0.03	0.01	0.02
La	0.02	0.02	0.02	0.03	0.02	0.03	0.03	0.03	0.04	0.02	0.03
Ce	0.03	0.05	0.04	0.05	0.04	0.05	0.06	0.06	0.07	0.05	0.06
Pr	0.01	0.00	0.00	0.00	0.01	0.00	0.00	0.02	0.01	0.00	0.01
Nd	0.02	0.02	0.02	0.01	0.01	0.02	0.02	0.02	0.02	0.02	0.02
Ca	1.47	1.50	1.45	1.55	1.61	1.69	1.70	1.66	1.65	0.87	1.72
K	0.03	0.03	0.03	0.03	0.03	0.05	0.05	0.05	0.04	0.07	0.04

[#] Refers to samples from the Geological Survey of Denmark and Greenland (GGU) collections.
Sample numbers 59661, 59663, eudialyte-bearing pegmatite, South Qôroq centre; DAR24, DAR26 - lujavrite in unit SN1B.
[+] metasomatically altered eudialyte rim
n.d. = not determined; < below detection limit.
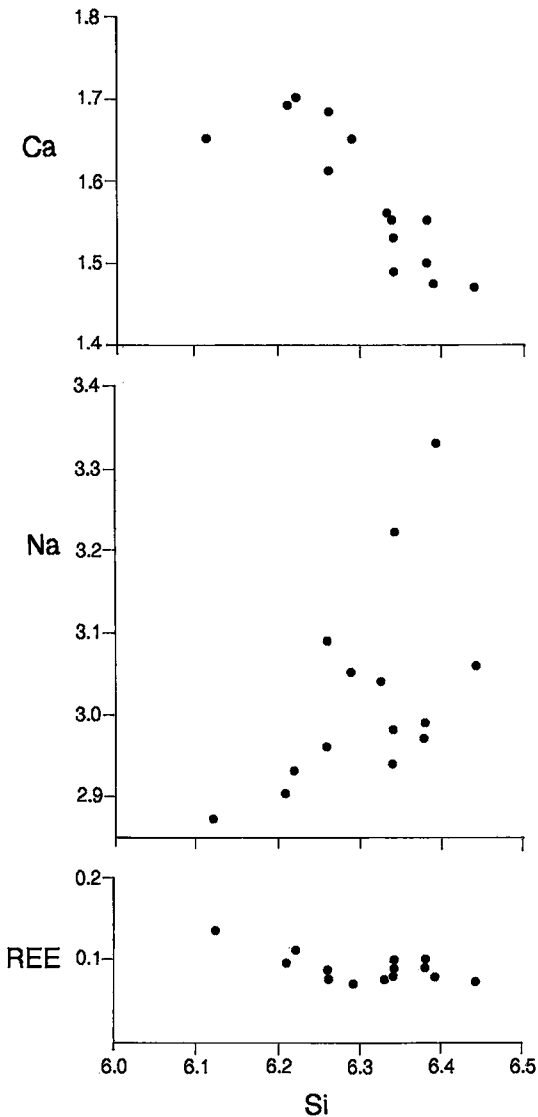
FIG. 6. Variation in levels of Ca, Na and *REE* for eudialyte, plotted against proportion of Si. Axes are plotted in cations per formula unit.

co-ordination sites (Ca) as outlined below.

The titanite shows significant departure from the ideal formula CaTi[SiO₄](O,OH,F). Samples may contain significant amounts of Zr (up to 2 wt.% ZrO₂), Al (2.5% Al₂O₃), Fe (3% Fe₂O₃), *REE* (2% *REE*₂O₃) and Nb (3% Nb₂O₅). Minor amounts of Na, Mn, Y and Th also are present, together with up to 0.5 wt.% F.

Na and *REE* (+ Y) substitute for Ca in the seven-fold co-ordinated site, and Al and Fe for Ti in the octahedral site, with only minor Al in the tetrahedral site (Deer *et al.* 1992). The site preference for Nb and Zr is less certain, but may be the octahedral site (Woolley *et al.* 1992). This arrangement gives good totals for occupancies of individual sites. The occupancy of the octahedral site is demonstrated quite convincingly in Figure 8, where Ti is plotted against other likely occupants. Data taken from the literature (Clark 1974, Woolley *et al.* 1992), showing greater degrees of substitution for Ti in the octahedral site, are included for comparison.

Niobium-rich varieties of titanite have been described by a number of authors (*e.g.*, Clark 1974, Woolley *et al.* 1992). Those described by Woolley *et al.* are associated with eudialyte in nepheline syenite pegmatite from northern Malawi, in a petrologically similar environment to North Qôroq, in which Nb is concentrated in the primary melt. *REE*-enriched titanite also is fairly common (Exley 1980, Nakada 1991), where again the elevated *REE* concentrations are due to primary magmatic processes. In and around North Qôroq, titanite shows variable degrees of enrichment in Nb, *REE* and Zr. Similar compositions of titanite were described by Russell *et al.* (1994) from Mount Bisson, British Columbia, where it occurs in both magmatic and metasomatic rocks. As noted above, titanite from North Qôroq is inferred to be metasomatic in origin, and this implies the existence of a fluid capable of transporting these elements. The distinct grouping of compositions, as seen in Figure 8, shows that for each sample, the titanite has a unique occupancy of the octahedral site. Contrasts are also apparent in the Ca and Si values. This suggests that the composition of titanite was partly controlled by the composition of the metasomatizing fluids and partly by the pre-existing composition and mineralogy of the protolith. For example, titanite formed around pre-existing grains of Fe–Ti oxide in the syenites tends to be more Ti-rich. Hence, although the composition of all grains of titanite was affected by the infiltrating fluid, not all completely equilibrated with it, and thus the solid phases were, at least locally, not completely buffered by this fluid.

Rare-earth fluorcarbonate minerals

Rare-earth fluorcarbonate phases only become clearly visible if the sample is viewed under BSEI, where the high concentrations of *REE* result in bright images. These phases are only evident in metasomatized rocks, where they occur as tiny poikiloblastic crystals (up to 20 μm) in association with carbonate and fluorite. They are volumetrically less important than the apatite, eudialyte and titanite, but their high *REE* contents mean that they play an important part in control of the overall *REE* profile of
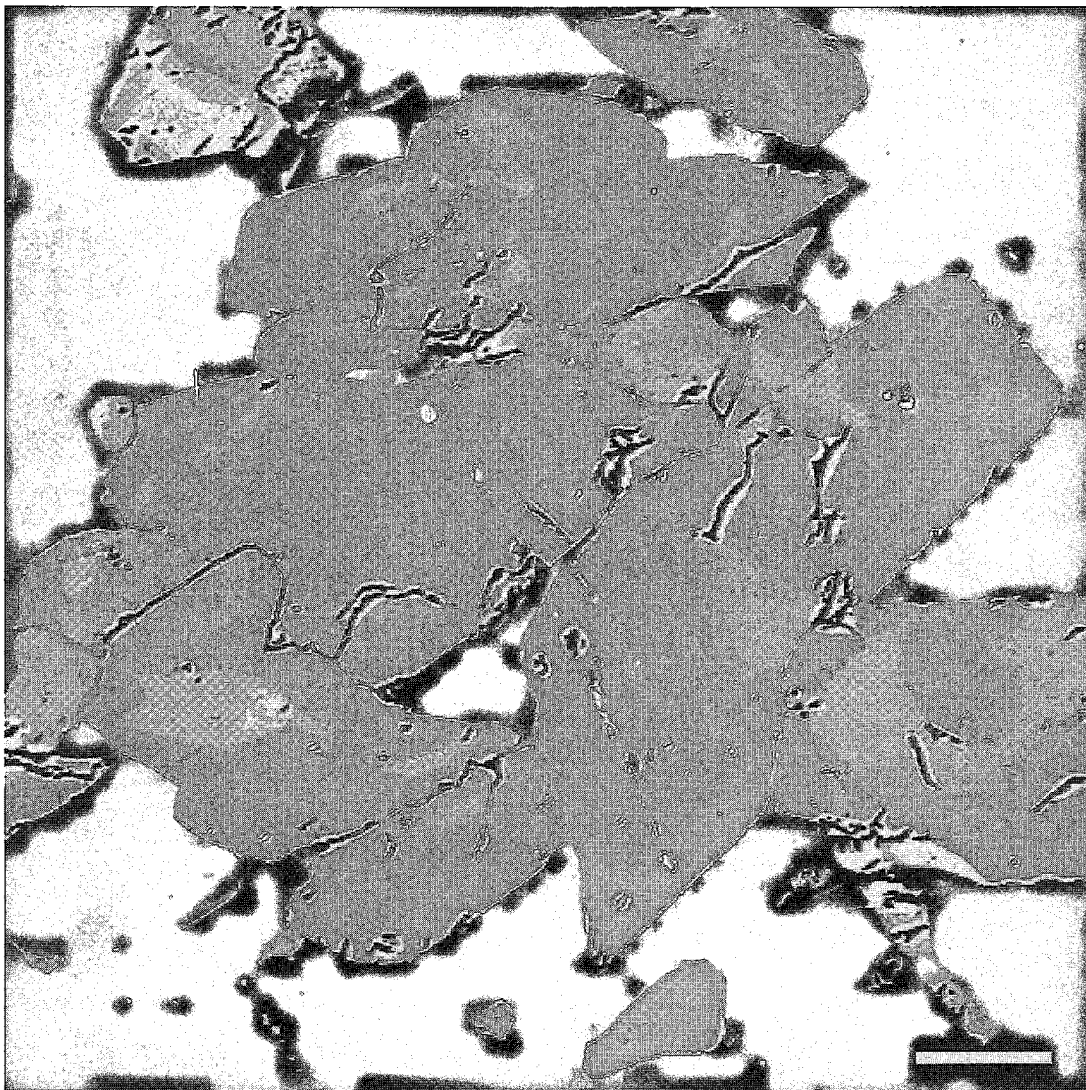
FIG. 7. BSEI of light-rare-earth-element-enriched titanite, showing detailed patterns of zonation due to differences in mean atomic number and rare-earth-element content in sample GGU52279 from the fenitized granite around the North Qôroq center. Surrounding material is alkali feldspar and quartz. Scale bar represents 50 μm.

the rocks.

The composition of these fluorcarbonate minerals suggests that they commonly occur as intergrowths involving synchysite $(REE)Ca(CO_3)_2F$, parisite $REE_2Ca(CO_3)_3F_2$ and bastnäsite $(REE)(CO_3)F$. Table 4 shows representative partial compositions of these phases (22 analyses were made on 8 grains from two samples). The lowest *REE* abundances are in synchysite but, even in this phase, the total proportion of *REE* oxides commonly exceeds 50 wt.%. Separate analyses of bastnäsite were not possible, as it occurs as an intimate fine-scale intergrowth with parisite.

DISCUSSION

Various patterns of zonation are apparent in the *REE*-bearing phases of North Qôroq. The simple concentric patterns seen in apatite and the regular oscillatory zoning in eudialyte, both occurring in syenitic rocks, are interpreted to be primary growth-features of the minerals, formed when these phases were in equilibrium with syenitic magma. Titanite is not a primary phase in the syenites; consequently, simple patterns may be due to growth during an initial single phase of metasomatism, with modification by

TABLE 3. REPRESENTATIVE RESULTS OF ELECTRON-MICROPROBE ANALYSES OF TITANITE FROM NORTH QÔROQ

Sample No.	DAR228 core	DAR234 core	DAR234 rim	DAR234 core	DAR234 rim	52279[#] middle	52279[#] middle	52279[#] rim	IMC17 core	IMC17 core
Oxide wt.%	1	2	3	4	5	6	7	8	9	10
SiO_2	28.91	29.81	29.70	29.97	29.92	29.57	29.54	29.60	30.15	29.61
TiO_2	30.14	34.69	35.47	35.13	35.01	39.30	37.54	37.96	35.91	36.14
ZrO_2	1.35	0.17	0.10	0.13	0.16	0.15	0.47	0.21	0.17	0.26
Al_2O_3	2.43	1.68	1.44	1.60	1.36	<	0.20	0.18	1.42	1.48
Fe_2O_{3total}	2.62	2.70	2.53	2.85	3.01	0.56	0.79	0.57	1.55	1.51
MnO	0.13	<	<	<	<	<	<	<	<	<
La_2O_3	0.44	<	<	<	0.11	0.22	0.21	0.18	0.13	<
Ce_2O_3	1.32	0.21	0.20	0.19	0.21	0.67	0.82	0.89	0.33	0.15
Nd_2O_3	0.39	0.13	0.11	<	<	0.39	0.72	0.76	0.17	<
Y_2O_3	0.44	<	<	<	<	<	0.22	0.27	0.10	0.12
Nb_2O_5	2.48	0.33	0.12	0.18	0.31	0.21	0.86	0.75	<	<
CaO	26.63	28.64	28.92	28.98	28.23	26.35	25.48	25.26	28.54	28.61
Na_2O	0.09	n.d.	n.d.	<	0.16	1.12	1.29	1.37	<	<
F	n.d.	0.36	0.23	n.d.	n.d.	n.d.	n.d.	n.d.	n.d.	n.d.
- O ≡ F	-	0.15	0.10	-	-	-	-	-	-	-
Total	97.36	98.57	98.72	99.03	98.48	98.53	98.14	98.00	98.47	97.88

Atomic proportions on the basis of 5 atoms of oxygen

Si	0.97	1.01	1.00	1.01	1.01	1.00	1.00	1.00	1.02	1.00
^{iv}Al	0.03	-	-	-	-	-	-	-	-	-
Σ	1.00	1.01	1.00	1.01	1.01	1.00	1.00	1.00	1.02	1.00
^{vi}Al	0.07	0.07	0.06	0.06	0.05	-	0.00	0.01	0.06	0.06
Ti	0.76	0.88	0.90	0.89	0.89	1.00	0.95	0.96	0.91	0.92
Fe^{3+}	0.07	0.07	0.06	0.07	0.08	0.01	0.02	0.01	0.04	0.04
Nb	0.04	0.01	0.00	0.00	0.00	0.00	0.01	0.01	0.00	0.00
Zr	0.02	0.00	0.00	0.00	0.00	0.00	0.01	0.00	0.00	0.00
Σ	0.96	1.02	1.02	1.03	1.03	1.02	1.00	1.00	1.01	1.02
Ca	0.96	1.03	1.04	1.05	1.02	0.95	0.92	0.91	1.03	1.03
Na	0.01	-	-	0.01	0.01	0.07	0.08	0.09	0.00	0.00
Ce	0.03	0.00	0.00	0.00	0.00	0.01	0.01	0.01	0.00	0.00
Σ	1.00	1.04	1.05	1.05	1.03	1.03	1.02	1.01	1.04	1.04
F	-	0.04	0.02	-	-	-	-	-	-	-

[#] Refers to samples from the Geological Survey of Denmark and Greenland (GGU) collections.
Sample No. DAR234, DAR228 & IMC17 metasomatised sediment, basalt and granite-gneiss near to unit SN1A;
52279 metasomatised granite-gneiss adjacent to the North Qôroq syenite.
n.d. = not determined; < below detection limits.

later events. Gieré & Williams (1992) described a similar occurrence of titanite from hydrothermal veins around the Adamello batholith, in Italy. Titanite in our study shows a simple, regular but discontinuous core-to-rim variation, but with the rim locally showing additional complex patterns. There is a likely alternative to a complete metasomatic origin for country-rock titanite: this simple pattern of zonation may indicate that the core zone is the remnant of original titanite that underwent later metasomatic replacement and growth, particularly around the margin.

The rather chaotic and irregular zonation, particularly well developed toward the margin of crystals, is a feature of apatite, titanite and eudialyte from the North Qôroq center. These patterns are easily identified using CL (apatite) and BSEI. The irregular nature, with cross-cutting relationships and lobate embayments of earlier growth-zones, together with the resorption at the edge of many crystals, indicate that metasomatic dissolution, alteration and reprecipitation occurred in these minerals. Analyses show that these irregular zones are internally chemically homogeneous. In some grains of apatite and eudialyte, several zones can be seen within a crystal, each with distinctive chemistry. The contrasts in brightness that render the zoning visible under BSEI are due primarily to variations in *REE* content. Similarly, the contrasting luminescence colors in apatite reflect varying concentrations of *REE*. Mariano & Ring (1975) advocated activation by Eu, with minor effects produced by other *REE*. Hayward & Jones (1991) proposed Eu^{2+} and Eu^{3+} activation to explain blue- and purple-luminescing apatite from extrusive carbonatite lavas close to the North Qôroq center. Exactly comparable luminescence colors are seen in the metasomatic apatite at North Qôroq, with zones ranging from blue to purple through shades of lilac. These zones within a crystal are the result of multiple metasomatic events associated with the emplacement and evolution of adjacent syenite units. When within a few tens of meters of a younger unit, or where the
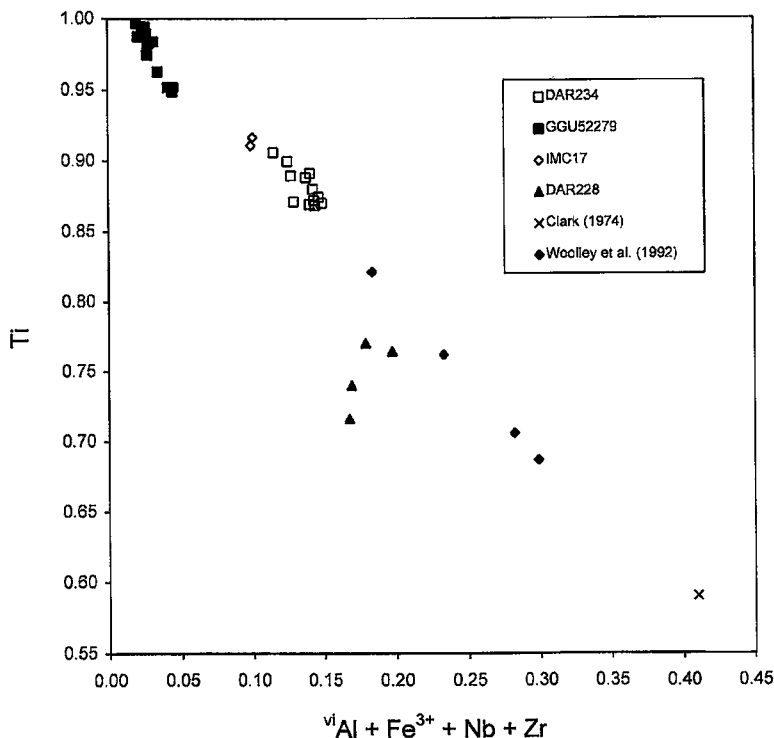
FIG. 8. Titanite substitution represented in terms of proportions of Ti *versus* ^{vi}Al + Fe^{3+} + Nb + Zr for North Qôroq titanite. Axes are plotted in cations per formula unit. Each rock sample is indicated by a different symbol. The range of compositions, and clustering of analyses for a particular sample, indicate a distinctive octahedral site-chemistry for each.

metasomatized rock is a xenolith, the effect is to produce zones with high *REE* concentrations. The greater the distance from the source of the metasomatic fluid, the weaker the metasomatic effect and the lower the influx of *REE*.

Strong Na-metasomatism is apparent both in and around the North Qôroq syenites and resulted in extensive albitization and the development of sodic minerals such as albite and poikiloblastic aegirine, alkali amphibole and aenigmatite. However, there is no evidence that such areas are *REE* enriched, and apatite and titanite are generally absent. Only eudialyte contains significant *REE*, occurs in association with sodic phases, and is itself Na-rich. This mineral is attributed to crystallization from a primary Na-rich magmatic liquid rather than being a product of metasomatism.

The analyses of both apatite and titanite show significant *REE* and minor Y, together with the presence of F. Zirconium and Nb also are present in titanite, and both these elements show evidence of mobility in the altered Ca-enriched rim of eudialyte grains. Apatite and titanite occur in veins and patches

that are dominated by calcite and fluorite, with other subordinate Ca-rich phases in and adjacent to these patches, including calcic amphibole, calcic pyroxene, hydrogrossular–andradite garnet and fluorcarbonates.

TABLE 4. REPRESENTATIVE RESULTS OF PARTIAL ELECTRON MICROPROBE ANALYSES OF FLUORCARBONATE MINERALS FROM NORTH QÔROQ

Sample No.	DAR67	DAR67	DAR67	DAR67	DAR67	DAR67	DAR65
	syn	syn	syn	syn	syn	par	par
Oxide wt.%	1	2	3	4	5	6	7
CaO	17.16	17.54	18.17	17.68	18.89	8.42	9.79
SrO	<	<	0.23	0.14	1.03	0.68
La$_2$O$_3$	16.60	17.31	14.18	13.38	12.82	15.31	15.28
Ce$_2$O$_3$	22.64	20.98	21.91	24.46	23.53	25.97	29.76
Pr$_2$O$_3$	2.24	2.13	2.13	2.69	2.58	2.77	3.09
Nd$_2$O$_3$	8.00	7.89	7.78	9.58	10.01	10.01	12.09
Sm$_2$O$_3$	0.87	0.79	0.97	0.91	1.30	1.46	1.18
Y$_2$O$_3$	0.51	0.65	0.83	0.52	1.01	1.46	0.13
ThO$_2$	n.d.	n.d.	n.d.	1.32	<	2.93	0.19
F	5.00	4.26	4.62	6.00	6.08	4.29	7.39
Total	73.01	71.56	70.57	76.78	76.36	73.64	79.58

Sample numbers DAR65, DAR67 metasomatised quartzite raft in syenite unit SN1B
syn = synchysite; par = parisite
n.d. = not determined; < below detection limit

We conclude that the metasomatic fluid responsible for the formation of apatite, titanite and fluorcarbonate, and for alteration of eudialyte along its rim, must have been capable of transporting the high-field-strength elements, Y and *REE*. Considerable evidence, both experimental and geological, has demonstrated that these elements can be readily mobilized under certain conditions, in a variety of environments and over a range of temperatures (*e.g.*, Martin *et al.* 1978, Hole *et al.* 1992). The most likely explanation is that these elements bond with ligands such as fluoride, carbonate, fluorcarbonate or phosphate, and are transported as complexes (Humpries 1984, Gieré & Williams 1992, Rubin *et al.* 1993, Pan *et al.* 1993).

The fluid responsible for the *REE* mobility is of probable carbonatitic affinity; its origin needs to be assessed. There are a variety of carbonatitic bodies adjacent to North Qôroq, including lava flows, dykes and carbonate breccia plugs, one of which cuts the center. However, the multiple zonation patterns seen in the apatite argue against a direct link with a carbonatitic parent, as there is no evidence of repeated carbonatitic magmatism affecting North Qôroq. Many of the altered syenites are distant from any obvious carbonatite sources, although the possibility of such bodies occurring at depth, below current levels of exposure, cannot be discounted.

What does occur as multiple events is the intrusion of the sequence of syenites constituting the North Qôroq center. Indeed, there is good correlation between the number of compositionally distinct zones seen in apatite crystals and the number of adjacent, younger syenite units. It seems likely that fluids of carbonatitic affinity, responsible for *REE* mobility, evolved from individual syenite units. Support for this comes from the carbonate-rich nature of the more evolved syenites, where cancrinite is a significant phase, with modal proportions up to 10%.

The association of Na-rich nepheline syenites with Ca-rich carbonatites is not exceptional. Similar associations have been described from, amongst other locations, the Juquiá Complex, Brazil (Beccaluva *et al.* 1992) and the Fen Complex, Norway (Andersen 1988), and a genetic link between the two rock types advocated.

The origin of carbonatites have been extensively studied over recent years (Wyllie *et al.* 1990); an origin for the metasomatizing "carbonatitic" fluid at North Qôroq by liquid immiscibility at shallow crustal level is entirely feasible. Early experimental work (Koster van Groos & Wyllie 1968, 1973) demonstrated a significant miscibility gap between carbonate and silicate liquids with Na-rich compositions. More recent work (Kjarsgaard & Hamilton 1988, 1989, Hamilton & Kjarsgaard 1993) has shown that, over a range of pressures, $CaCO_3$-rich carbonatite melts can readily form by liquid immiscibility from peralkaline silicate parent magmas. The CO_3^{2-}-rich fluid responsible for

REE mobility in and around the North Qôroq center is similarly considered to have separated as an immiscible liquid from evolved nepheline syenite magma at a shallow level in the crust.

CONCLUSIONS

The study of *REE*-bearing phases in and around the North Qôroq center has resulted in the following conclusions relevant to the behavior of *REE* and the nature of the metasomatizing fluids.
1. Mineral zonation is revealed optically, and with CL and BSEI. Where simple, this zonation probably reflects primary magmatic growth. Where it follows a complex pattern, with embayments and cross-cutting relationships, it is attributed to a series of multiple metasomatic events that have altered the mineral's composition.
2. Apatite, titanite and eudialyte show variation in mineral chemistry. This involves the *REE* and, in some cases, other elements, such as, Zr, Nb and Y. Transport of these elements has occurred *via* a metasomatizing fluid phase.
3. The fluid responsible for *REE*-metasomatism was Ca-, F^--, CO_3^{2-}- and PO_4^{3-}-rich, with carbonatitic affinities, and evolved from individual batches of syenitic magma at a late stage in their development, probably by a process of liquid immiscibility. It contrasts with the residual peralkaline magmatic liquids, which were extremely Na-rich, and also with a Na-rich aqueous phase separating from the syenitic magma at an earlier stage.

REFERENCES

ANDERSEN, T. (1988): Evolution of peralkaline calcite carbonatite magma in the Fen complex, southeast Norway. *Lithos* **22**, 99-112.

BECCALUVA, L., BARBIERI, M., BORN, H., BROTZU, P., COLTORTI, M., CONTE, A., GARBARINO, C., GOMES, C.B., MACCIOTTA, G., MORBIDELLI, L., RUBERTI, E., SIENA, F. & TRAVERSA, G. (1992): Fractional crystallization and liquid immiscibility processes in the alkaline-carbonatite complex of Juquiá (São Paulo, Brazil). *J. Petrol.* **33**, 1371-1404.

BLAXLAND, A.B., VAN BREEMEN, O., EMELEUS, C.H. & ANDERSON, J.G. (1978): Age and origin of the major syenite centres in the Gardar province of South Greenland: Rb–Sr studies. *Geol. Soc. Am., Bull.* **89**, 231-244.

CHAMBERS, A.D. (1976): *The Petrology and Geochemistry of the North Qôroq centre, Igaliko Complex, South Greenland.* Ph.D. thesis, Univ. of Durham, Durham, U.K.

CLARK, A.M. (1974): A tantalum-rich variety of sphene. *Mineral. Mag.* **39**, 605-607.

DEER, W.A, HOWIE, R.A. & ZUSSMAN, J. (1992): *An Introduction to the Rock-Forming Minerals* (2nd ed.). Longman Scientific & Technical, Harlow, England.

DRAKE, M.J. & WEILL, D.F. (1972): New rare earth element standards for electron microprobe analysis. *Chem. Geol.* **10**, 179-181.

EMELEUS, C.H. & HARRY, W.T. (1970): The Igaliko nepheline syenite complex: general description. *Meddr. Grønland* **186**(3).

EXLEY, R.A. (1980): Microprobe studies of *REE*-rich accessory minerals: implications for Skye granite petrogenesis and *REE* mobility in hydrothermal systems. *Earth Planet. Sci. Lett.* **48**, 97-110.

GIERÉ, R. & WILLIAMS, C.T. (1992): *REE*-bearing minerals in a Ti-rich vein from the Adamello contact aureole (Italy). *Contrib. Mineral. Petrol.* **112**, 83-100.

GIUSEPPETTI, G., MAZZI, F. & TADINI, C. (1971): The crystal structure of eudialyte. *Tschermaks Mineral. Petrogr. Mitt., Ser. 3,* **16**, 105-127.

HAMILTON, D.L. & KJARSGAARD, B.A. (1993): The immiscibility of silicate and carbonate liquids. *S. Afr. J. Geol.* **96**(3), 139-142.

HARRIS, C. & RICKARD, R.S. (1987): Rare-earth-rich eudialyte and dalyite from a peralkaline granite dyke at Straumsvola, Dronning Maud Land, Antartica. *Can. Mineral.* **25**, 755-762.

HAYWARD, C.L. & JONES, A.P. (1991): Cathodoluminescence petrography of Middle Proterozoic extrusive carbonatite from Qasiarsuk, South Greenland. *Mineral. Mag.* **55**, 591-603.

HOLE, M.J., TREWIN, N.H. & STILL, J. (1992): Mobility of high field strength, rare earth elements and yttrium during late diagenesis. *J. Geol. Soc.* **149**, 689-692.

HUMPHRIES, S.E. (1984): The mobility of the rare earth elements in the crust. *In* Rare Earth Element Geochemistry (P. Henderson, ed.). Elsevier, Amsterdam, The Netherlands (317-342).

JONES, A.P. (1980): *The Petrology and Structure of the Motzfeldt Centre, Igaliko, South Greenland.* Ph.D. thesis, Univ. of Durham, Durham, U.K.

_____ & LARSEN, L.M. (1985): Geochemistry and *REE* minerals of nepheline syenites from the Motzfeldt Centre, South Greenland. *Am. Mineral.* **70**, 1087-1100.

KJARSGAARD, B.A. & HAMILTON, D.L. (1988): Liquid immiscibility and the origin of alkali-poor carbonatites. *Mineral. Mag.* **52**, 43-55.

_____ & _____ (1989): The genesis of carbonatites by liquid immiscibility. *In* Carbonatites: Genesis and Evolution (K. Bell, ed.). Unwin Hyman, London, U.K. (388-404).

KOSTER VAN GROOS, A.F. & WYLLIE, P.J. (1968): Liquid immiscibility in the join $NaAlSi_3O_8 - Na_2CO_3 - H_2O$ and its bearing on the genesis of carbonatites. *Am. J. Sci.* **266**, 932-967.

_____ & _____ (1973): Liquid immiscibility in the join $NaAlSi_3O_8 - CaAlSi_2O_8 - Na_2CO_3 - H_2O$ and its bearing on the genesis of carbonatites. *Am. J. Sci.* **273**, 465-487.

MACDONALD, R. & UPTON, B.G.J. (1993): The Proterozoic Gardar rift zone, South Greenland: comparisons with the East African Rift System. *In* Magmatic Processes and Plate Tectonics (H.M. Prichard, T. Alabaster, N.B.W. Harris & C.R. Neary, eds.). *Geol. Soc., Spec. Publ.* **76**, 427-442.

MARIANO, A.N. & RING, P.J. (1975): Europium-activated cathodoluminescence in minerals. *Geochim. Cosmochim. Acta* **39**, 649-660.

MARTIN, R.F., WHITLEY, J.E. & WOOLLEY, A.R. (1978): An investigation of rare earth mobility: fenitised quartzites, Borralan Complex, N.W. Scotland. *Contrib. Mineral. Petrol.* **66**, 69-73.

NAKADA, S. (1991): Magmatic processes in titanite-bearing dacites, central Andes of Chile and Bolivia. *Am. Mineral.* **76**, 548-560.

PAN, YUANMING, FLEET, M.E. & MACRAE, N.D. (1993): Late alteration in titanite ($CaTiSiO_5$): redistribution and remobilization of rare earth elements and implications for U/Pb and Th/Pb geochronology and nuclear waste disposal. *Geochem. Cosmochim. Acta* **57**, 355-367.

POUCHOU, J.L & PICHOIR, F. (1984): A new model for quantitative X-ray microanalyses. I. Application to the analysis of homogenous samples. *La Recherche Aérospatiale* **3**, 13-38.

RAE, D.A. & CHAMBERS, A.D. (1988): Metasomatism in the North Qôroq centre, South Greenland: cathodoluminescence and mineral chemistry of alkali feldspars. *Trans. R. Soc. Edinburgh, Earth Sci.* **79**, 1-12.

————, COULSON, I.M. & CHAMBERS, A.D. (1996): Metasomatism in the North Qôroq centre, South Greenland: apatite chemistry and rare-earth element transport. *Mineral. Mag.* **60**, 207-220.

RØNSBO, J.G. (1989): Coupled substitutions involving *REE*s, Na and Si in apatites in alkaline rocks from the Ilímaussaq intrusion, South Greenland, and the petrological implications. *Am. Mineral.* **74**, 896-901.

RUBIN, J.N., HENRY, C.D. & PRICE, J.G. (1993): The mobility of zirconium and other "immobile" elements during hydrothermal alteration. *Chem. Geol.* **110**, 29-47.

RUSSELL, J.K., GROAT, L.A. & HALLERAN, A.A.D. (1994): *LREE*-rich niobian titanite from Mount Bisson, British Columbia: chemistry and exchange mechanisms. *Can. Mineral.* **32**, 575-587.

STORMER, J.C., JR., PIERSON, M.L. & TACKER, R.C. (1993): Variation in F and Cl X-ray intensity due to anisotropic diffusion in apatite during electron microprobe analysis. *Am. Mineral.* **78**, 641-648.

UPTON, B.G.J. & EMELEUS, C.H. (1987): Mid-Proterozoic alkaline magmatism in southern Greenland. *In* Alkaline Igneous Rocks (J.G. Fitton & B.G.J. Upton, eds.). *Geol. Soc., Spec. Publ.* **30**, 449-471.

WOOLLEY, A.R., PLATT, R.G. & EBY, N. (1992): Niobian titanite and eudialyte from the Ilomba nepheline syenite complex, north Malawi. *Mineral. Mag.* **56**, 428-430.

WYLLIE, P.J., BAKER, M.B. & WHITE, B.S. (1990): Experimental boundaries for the origin and evolution of carbonatites. *Lithos* **26**, 3-19.